ChemComm

Accepted Manuscript

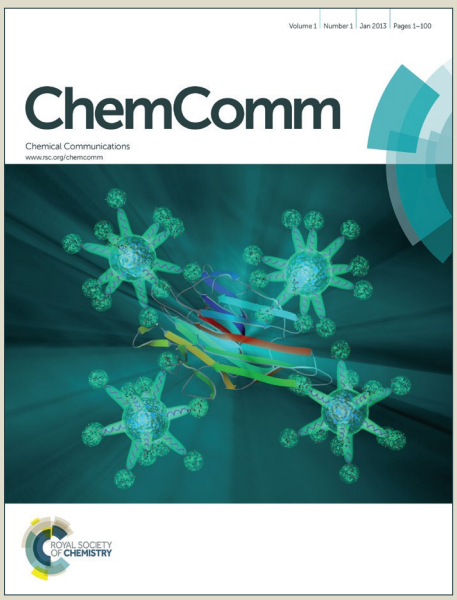

ROYAL SOCIETY OF CHEMISTRY

www.rsc.org/chemcomm

Journal Name

COMMUNICATION

Nucleus-staining with biomolecule-mimicking nitrogen-doped carbon dots prepared by fast neutralization heat strategy

Received 00th January 20xx,
Accepted 00th January 20xx

DOI: 10.1039/x0xx00000x

www.rsc.org/

Yan-Fei Kang,[a,†] Yang-Wu Fang,[b,†] Yu-Hao Li,[b] Wen Li,[b] and Xue-Bo Yin[a,*]

Biomolecule-mimicking nitrogen-doped carbon dots (N-Cdots) were synthesized from dopamine by neutralization heat strategy. Fluorescence imaging of various cells validated their nucleus-staining efficiency. The dopamine-mimicking N-Cdots "tricks" nuclear membrane to achieve the nuclear localization and imaging.

Cell is an important carrier in the process of life. Research for the interaction between cell and xenobiotics helps us understanding their transportation, metabolism and toxicity.[1] Cell nucleus is critical to various important cellular events, including metabolism, heredity, and reproduction.[1] However, the research on cell nucleus is deficient comparing with its vital significance.[2] Nucleus-staining is the first step to reveal the nucleus morphology, to investigate the nuclear function and to transfer the agent to cell nucleus.[3] Fluorescence nucleus-staining is popular because of its visualization and high resolution along with the fast development of fluorescence microscopy.[4] To overcome the drawbacks of self-quenching and photo-bleaching of some dyes, such as 4',6-diamidino-2-phenylindole (DAPI) and Hoechst stains, transition metal complexes have been developed with high luminescence efficiency, tunable emission color, large Stokes shift, and high photo-stability to enhance the nucleus-staining efficiency.[5] With careful design and complex preparation procedure, various nucleus-staining complexes have been reported, but DNA intercalation of complexes interferes with the DNA function.[5] So, it is critical to develop the nucleus-staining agent with simple procedure, high luminescence efficiency, low cytotoxicity and high photo-stability.

Nitrogen-doped carbon dots (N-Cdots) show the distinctive characteristics, such as stability, low toxicity and good biocompatibility.[6] Their fluorescence properties make N-Cdots extensive applications as sensing and fluorescence imaging probe.[6] However, the *in vitro* fluorescence imaging always shows that it is cytoplasm but not nucleus to be stained possibly because of the powerful defensive function of nuclear membrane.[6c, 7] An alternative strategy should be developed to prepare nucleus-staining N-Cdots with simple procedure. Dopamine is extensively studied by its polymerization ability to form polydopamine (PDA).[7,8] PDA has been applied for cell imaging,[9] anti-cancer drug delivery,[10] metal ion detection[11] and biosensing by its high biocompatibility.[12]

Here, we proposed a strategy to prepare biomolecule-mimicking N-Cdots as potential nucleus-staining agent. To this end, a fast neutralization heat strategy was used.[13] The neutralization heat released from ethylenediamine and phosphoric acid achieved the formation of N-Cdots with dopamine as precursor within 2 min. Cell imaging of Cdots validated their nucleus-staining efficiency with four kinds of cancer cells as models. The flow chart for the synthesis of N-Cdots was presented as Scheme S1.

The active hydroxyl group in dopamine facilitates the formation of carbon core via inducing the intermolecular condensation with the help of neutralization heat, similar to the polymerization of dopamine.[14] The further dehydration and carbonization achieves the formation of N-Cdots;[12] neutralization heat strategy does not require any expensive equipment and phosphoric acid has low volatility and corrosiveness for the sake of safety.[13] Moreover, the fast neutralization heat strategy provides a chance to prepare dopamine-mimicking N-Cdots as illustrated followed.

The as-prepared N-Cdots were characterized with Fourier transform infrared (FTIR), X-ray photoelectronic spectroscopy (XPS) and transmission electron microscope (TEM) images. The broad and intense peaks at 3362 cm^{-1} and the peak at 1284 cm^{-1} in FTIR spectrum are attributed to C-OH stretching and -OH bending vibration (Fig. 1a). The peaks at 1611 and 1520 cm^{-1} are related to the bending vibration of N-H (primary amine). The peak at 1342 cm^{-1} comes from the stretching vibration of the phenolic hydroxyl group on N-Cdots' surface. In XPS broad spectrum of N-Cdots, three peaks

[a] *Research Center for Analytical Sciences, College of Chemistry, Nankai University, Tianjin Key laboratory of Biosensing and Molecular Recognition, State Key Laboratory of Medicinal Chemical Biology, Collaborative Innovation Center of Chemical Science and Engineering (Tianjin), Tianjin 300071, China.*
[b] *Tianjin Key Laboratory of Tumor Microenviroment and Neurovascular Regulation, School of Medicine, Nankai University, Tianjin, 300071, China.*
* Correspondence should be addressed to X.B.Y. E-mail: xbyin@nankai.edu.cn; Fax: (+86) 022-23503034
† These authors contributed equally.
Electronic Supplementary Information (ESI) available: Materials and methods, full experimental and characterization details, MTT test, other CLSM images zeta potential and other fluorescence spectra. See DOI: 10.1039/x0xx00000x

at 284.7, 397.0, and 530.2 eV were attributed to C_{1s}, N_{1s} and O_{1s}, respectively (Fig. 1b). The calculated mass content of N and O element are 7.92% and 20.80%, respectively. So, the Cdots were successfully doped with nitrogen and therefore denoted as N-Cdots. The high oxygen content validated their good solubility. Fig. 1c-e shows the high-resolution XPS spectra of C_{1s}, N_{1s} and O_{1s}. C_{1s} spectrum was deconvolved into three peaks at 284.6 eV, 285.9 eV and 288.4 eV, corresponded to C-C, C-O and C=O/C=N bands, respectively (Fig. 1c). The results fit well with the FTIR data and illustrate that the N-Cdots surface was equipped with the functional groups, including -COOH, -OH and -NH_2. All of the results confirm the formation of N-Cdots from dopamine. The morphology and size distribution of N-Cdots illustrated their uniform dispersity. The size mainly focused on 2-3 nm with an average diameter of 2.34 nm (Fig. 2a-c). The lattice spacing of 0.24 nm validated the sp^2 cluster structure of N-Cdots by high resolution TEM image (Fig. 2b).[15]

The optical properties of N-Cdots were illustrated in Fig. 2d. The N-Cdots solution was transparent with light yellow while bright bluish green emission was observed under 365 nm light excitation. The absorption peak at 297 nm (Fig. 2d) is attributed to n-π* transition of C=O and π-π* transition of C=C.[11] With the excitation from 340 to 480 nm, the emission of N-Cdots shows little shifts and reveals the excitation-independent emission characteristic of N-Cdots. N-Cdots have a quantum yield of 5.2% (Table S1, ESI) and a fluorescence lifetime of 7.26 ns (Fig. S1 and Table S2, ESI). Moreover, high photostability was observed from N-Cdots as illustrated in Fig. S2, ESI.

The fluorescence imaging application of N-Cdots was first investigated with confocal laser scanning microscope with PC12 cells as model. N-Cdots were found in cytoplasm and the nucleus was also clearly observed (Fig. 3), different to the simple cytoplasm imaging of previous Cdots.[7,16] The brightness of PC12 cells increased with the N-Cdots concentration increasing, indicating the emission was from the Cdots embedded into the cells. As a comparison, no apparent brightness was observed in the control group. The result validated that N-Cdots entered into the cells successfully. N-Cdots are enclosed by cell membrane through endocytosis and entered into the cytoplasm to lighten cytoplasm. Moreover, nucleus was much brighter than cytoplasm, different to the dark nucleus reported previously.[7, 16] With increased N-Cdots concentration, the

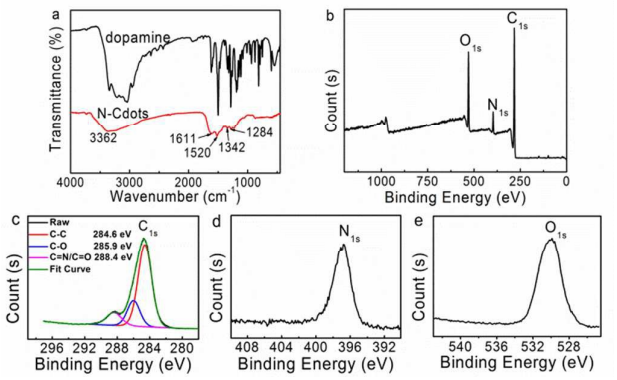

Fig. 1 (a) The FTIR spectra of dopamine and N-Cdots. (b) The broad XPS spectra of N-Cdots. The high-resolution XPS spectra of C1s (c), N1s (d) and O1s (e) of N-Cdots.

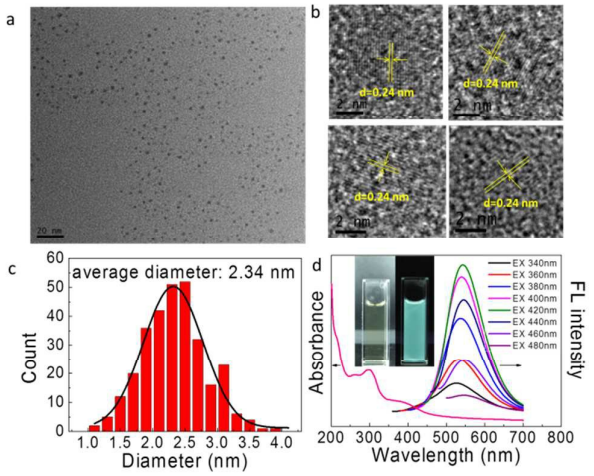

Fig. 2 (a) TEM and (b) HRTEM images of N-Cdots. (c) The particle size distribution of N-Cdots calculated from more than 200 particles and the fitting line. (d) UV-vis and fluorescence emission spectra of N-Cdots at the excitation wavelength from 340 to 480 nm. Inset: the photos of N-Cdots solution under white light (left) and UV light of 365 nm (right). Scale bars: 20 nm in TEM and 2 nm in HRTEM.

nucleus became brighter, illustrating their high affinity towards the nucleus. It is easy to understand the bright cytoplasm because of the small size of Cdots, similar to previous reports.[7, 16] Whether do our Cdots have a general nucleus-staining efficiency and why can they cross the nucleolemma and brighten the nucleus?

To validate the generalization of our N-Cdots as nucleus-staining agent, A549, HepG 2, and MD-MBA-231 cells were then selected as models to investigate the cellular uptake and distribution of N-Cdots. As illustrated in Fig. 4, A549, HepG 2, and MD-MBA-231 cells also have bright nucleus after incubating with N-Cdots, similar to PC12 cells (Fig. S3-S5, ESI). Overlap of the emission from N-Cdots and DAPI further confirmed the nuclear targeting of N-Cdots and N-Cdots were introduced into the cell nucleus (Fig. 4). So, our N-Cdots are a general nucleus-staining agent for those cells.

When A549 cells incubated with 0.8 or 1.0 mg mL^{-1} N-Cdots were monitored at different time, we found that the onset of cellular uptake was observed after 0.5 h, followed by a continuous increase in their brightness up to 12 h (Fig. 5 and Fig. S6 in ESI). The green fluorescence of N-Cdots was first observed in the cytoplasm around the nucleus. With incubation time increasing, the co-localization of blue fluorescence of DAPI and green fluorescence of N-Cdots suggested the nuclear internalization of N-Cdots. Different to the

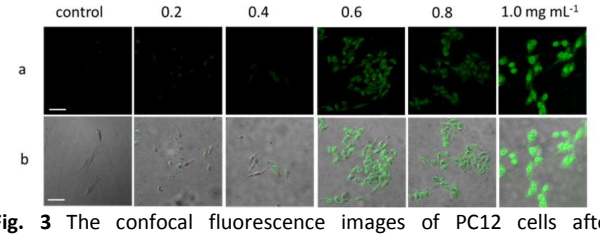

Fig. 3 The confocal fluorescence images of PC12 cells after incubating with proper medium contains 0, 0.2, 0.4, 0.6, 0.8 and 1.0 mg mL^{-1} of N-Cdots for 12 h: green fluorescence images (488 nm excitation and 500-540 nm emission) (a) and merge of the bright field and green fluorescence images (b). Scale bars: 30 μm.

simple nucleus-staining of DAPI, cytoplasmic constriction was clearly observed with the emission of N-Cdots. The cells kept good morphology, although the incubation time led to the dehydration of cells at high N-Cdots concentration. The result illustrated the low toxicity of N-Cdots. So, N-Cdots are took up through endocytosis and then cross the cell's nucleolemma to enter the nucleus, different to previous Cdots,[6b,7,12] but they do not affect cell growth.

The cell internalization of Cdots was strongly influenced by their size, surface charge, and groups. Our Cdots have the almost same small size to the other Cdots,[6b,7, 10-13] but their zeta potential was +12.8 mV (Fig. S7, ESI). So, our strategy provided the chance to synthesize positively charged N-Cdots, different to the previous methods.[6b,10-13] Positive charge favours and promotes the internalization of Cdots by electrostatic interaction to the negatively charged lipid membrane of cells and DNA in nucleus.[17] Amino groups on N-Cdots surface may be the only source for the positively charge, as validated by the high content of nitrogen in XPS spectrum. So, the neutralization heat strategy is obviously different to the previous hydrothermal and nitric acid refluxing procedure, where the negative surface charge of Cdots were obtained.[6b,7,12]

The other is the surface groups of Cdots. Because of the surface positive charge and high content of nitrogen, amino group exists on our N-Cdots' surface. Catechol groups exist in dopamine and can interact with Ag^+ ions and boric acid. So we test whether catechol group exists in the Cdots surface by their interaction with Ag^+ ions and boric acid. The fluorescence of N-Cdots was quenched by Ag^+ ions with high selectivity (Fig. S8, ESI). The quenching achieved by the interaction between Ag^+ ions and catechol groups on N-Cdots' surface. It was confirmed by the fluorescence recovery by cysteine with the high affinity between Ag^+ and cysteine (Fig. S9, ESI). The feasibility of detection of cysteine was confirmed in the Table S3 in ESI. The underlying nature of the selective detection of the Ag^+ ions and cysteine were tested in ESI. Boric acid was observed to enhance the fluorescence of N-Cdots. 20 % fluorescence enhancement was observed from Cdots when they were treated with 25 mM boric acid (Fig. S10, ESI). This result further illustrated that catechol groups existed on N-Cdots' surface for the interaction to boric acid. So, amino and catechol groups exist on the Cdots surface and their source could only be the incomplete carbonization of dopamine. While Ag^+ ions quench the fluorescence of Cdots by energy transfer, boric acid enhances their fluorescence because of the decreased surface defect through the interaction between boric acid and catechol group. So the fast neutralization heat strategy can keep the active groups of dopamine on N-Cdots' surface and we denoted our Cdots as biomolecule-mimicking Cdots. Their positive charge and small size make them cross the nuclear pore, with the size of 20–50 nm,[18] with the help of dopamine-mimicking structure.

The cytotoxicity of Cdots was first tested by MTT strategy, but higher than 100 % cell viability was observed at high concentration of Cdots similar to previous reports.[7,19] Moreover, the cell viability increased with the increased Cdots concentration. We considered the soluble Cdots in DMSO interfere with the absorbance at 490 nm. So, flow cytometry was used and the "true" low cytotoxicity was observed with A549 cells mortality of 4.20 % even the cells were treated with 1.0 mg mL^{-1} N-Cdots (Fig. 6 and Fig. S11, ESI). The flow cytometry results illustrated that most of the A549 cells are non-apoptotic cells and early apoptotic cells (Fig. S12 and Table S4, ESI). So, the combination of small size, positive charge, dopamine-mimicking surface groups and low cytotoxicity make our Cdots suitable for nucleus-staining for various cells.

In summary, nucleus-staining carbon dots were prepared with one-step neutralization heat strategy with dopamine as precursor. Studies on nucleus-staining mechanism indicated that small size, surface positive charge and dopamine-mimicking groups of the Cdots are critical to their entrance into nucleus. So, while the neutralization heat strategy is fast and simple, it also provides a biomolecule-mimicking efficiency because of the short reaction time for incomplete carbonization of the precursor. The N-Cdots were taken up by PC12, A549, HepG 2, and MD-MBA-231 cells through endocytosis and then cross the nucleolemma to enter the nucleus for imaging application. So they are a promising candidate as nucleus-staining probe used in biology- and medicine-relevant research by their low toxicity, excellent photostability and biomolecule-mimicking property. Further surface modification of the N-Cdots may bring facility to new materials related to selective nucleus staining and location as a new nucleus targeting vector.

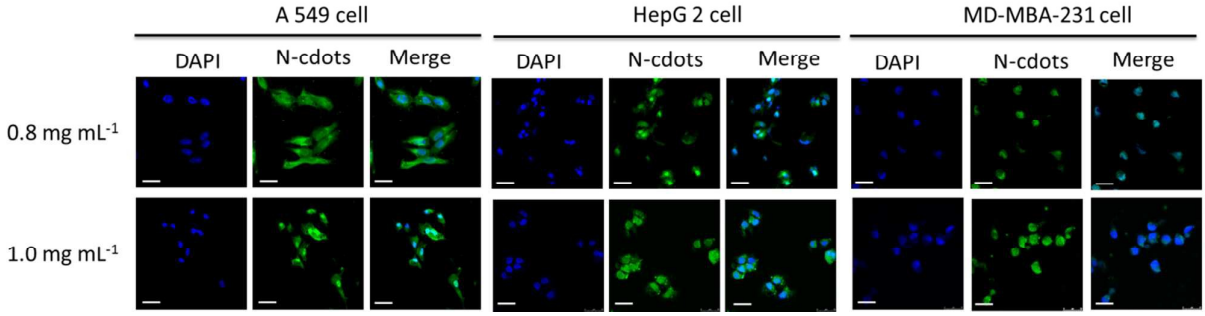

Fig. 4 The confocal fluorescence images of A549 cell, HepG 2 cell and MD-MBA-231 cell after incubating with medium contains 0.8 and 1.0 mg mL^{-1} of N-Cdots for 12 h: blue fluorescence images of nucleus stained with DAPI (405 nm excitation and 450–470 nm emission), green fluorescence images of N-Cdots in cells (488 nm excitation and 500–540 nm emission) and merge of the fluorescence images of nucleus and N-Cdots in cells. Scale bars: 30 μm.

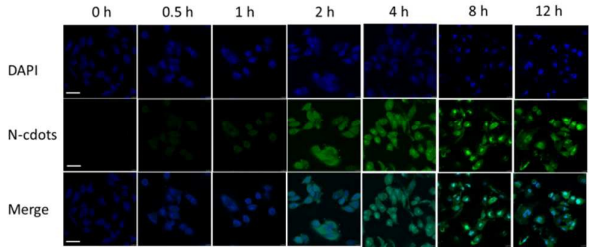

Fig. 5 The confocal fluorescence images of A549 cell after incubating with proper medium contains 1.0 mg mL^{-1} of N-Cdots at different time. Fluorescence nucleus-stained images with DAPI (405 nm excitation and 450–470 nm emission), green fluorescence images of N-Cdots (488 nm excitation and 500–540 nm emission) and their merge images. Scale bars: 30 μm.

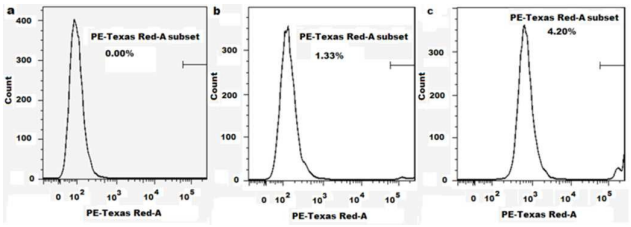

Fig. 6 Cytotoxicity of N-Cdots towards A549 cells measured by flow cytometry. (a) negative control used for select "gate" and A549 cells were incubated with (b) 0 (control) and (c) 1.0 mg mL^{-1} of N-Cdots for 12 h, respectively.

This work was supported by the National Natural Science Foundation of China (Grants 21075116 and 21190040) and 973 projects (2010CB933600 and 2011CB911000).

Notes and references

1 C. Y. Li, Y. Liu, Y. Q. Wu, Y. Sun and F. Y. Li, *Biomaterials*, 2013, **34**, 1223-1234.
2 A. Wragg, M. R. Gill, D. Turton, H. Adams, T. M. Roseveare, C. Smythe, X. Su and J. A. Thomas, *Chem. Eur. J.*, 2014, **20**, 14004-14011.
3 R. W. Horobin, J. C. Stockert and F. Rashid-Doubell, *Histochem. Cell Biol.*, 2013, **139**, 623-637.
4 (a) A. Nakamura, K. Takigawa, Y. Kurishita, K. Kuwata, M. Ishida, Y. Shimoda, I. Hamachi and S. Tsukiji, *Chem. Commun.*, 2014, **50**, 6149-6152; (b) A. S. Boutorine, D. S. Novopashina, O. A. Krasheninina, K. Nozeret and A. G. Venyaminova, *Molecules*, 2013, **18**, 15357-15397.
5 (a) J. X. Ru, X. L. Tang, Z. H. Ju, G. L. Zhang, W. Dou, X. Q. Mi, C. M. Wang and W. S. Liu, *Acs Appl. Mater. & Inter.*, 2015, **7**, 4247-4256; (b) E. Baggaley, M. R. Gill, N. H. Green, D. Turton, I. V. Sazanovich, S. W. Botchway, C. Smythe, J. W. Haycock, J. A. Weinstein and J. A. Thomas, *Angew. Chem. Int. Ed.*, 2014, **53**, 3367-3371; (c) D. Hara, H. Komatsu, A. Son, S. Nishimoto and K. Tanabe, *Bioconjugate Chem.*, 2015, **26**, 645-649
6 (a)W. P. Wang, Y. C. Lu, H. Huang, J. Feng, J. R. Chen and A. J. Wang, *Analyst*, 2014, **139**, 1692–1696; (b) Y. Xu, M. Wu, Y. Liu, X. Z. Feng, X. B. Yin, X. W. He, Y. K. Zhang, *Chem. Eur. J.* 2013, **19**, 2276 – 2283; (c) X. Y. Zha, P. Zhang, C. J. Liu, T. Ba, W. C Li, L. M. Dai and W. G. Liu, *Chem. Commun.*, 2012, **48**, 7955-7957;(d) Z. S. Qian, J. J. Ma, X. Y. Shan, H. Feng, L. X. Shao, and J. R. Chen, *Chem. Eur. J.* 2014, **20**, 2254-2263.
7 (a) X. Liu, J. Cao, H. Li, J. Li, Q. Jin, K. Ren and J. Ji, *Acs Nano*, 2013, **7**, 9384-9395; (b) W. B. Qiang, W. Li, X. Q. Li, X. Chen and D. K. Xu, *Chem. Sci*., 2014, **5**, 3018-3024.
8 Q. Ye, F. Zhou and W. Liu, *Chem. Soc. Rev.*, 2011, **40**, 4244-4258.
9 X. Y. Zhang, S. Q. Wang, L. X. Xu, L. Feng, Y. Ji, L. Tao, S. X. Li and Y. Wei, *Nanoscale*, 2012, **4**, 5581-5584.
10 C. C. Ho and S. J. Ding, *J. Mater. Sci-mater. M.*, 2013, **24**, 2381-2390.
11 K. G. Qu, J. S. Wang, J. S. Ren and X. G. Qu, *Chem-Eur. J.*, 2013, **19**, 7243-7249.
12 (a) S.-T. Yang, L. Cao, P. G. Luo, F. Lu, X. Wang, H. Wang, M. J. Meziani, Y. Liu, G. Qi and Y.-P. Sun, *J. Am. Chem. Soc.*, 2009, **131**, 11308-11309; (b) S. N. Baker and G. A. Baker, *Angew. Chem. Int. Ed.*, 2010, **49**, 6726-6744; (c) Y. Xu, X.-H. Jia, X.-B. Yin, X.-W. He and Y.-K. Zhang, *Anal. Chem.*, 2014, **86**, 12122-12129; (d) L. Cheng, Y. M. Li, X. Y. Zhai, B. Xu, Z. Q. Cao and W. G. Liu, *Acs Appl. Mater. & Inter*., 2014, **6**, 20487-20497; (e) H. Huang, C. G. Li, S. J. Zhu, H. L. Wang, C. L. Chen, Z. R. Wang, T. Y. Bai, Z. Shi and S. H. Feng, *Langmuir*, 2014, **30**, 13542-13548; (f) X. Y. Ji, F. Peng, Y. L. Zhong, Y. Y. Su and Y. He, *Colloid. Surface. B*, 2014, **124**, 132-139; (g) V. N. Mehta, S. Jha, R. K. Singhal and S. K. Kailasa, *New J. Chem.*, 2014, **38**, 6152-6160.
13 X. M. Wei, Y. Xu, Y. H. Li, X. B. Yin and X. W. He, *RSC Advances*, 2014, **4**, 44504-44508.
14 (a) H. Lee, S. M. Dellatore, W. M. Miller and P. B. Messersmith, *Science*, 2007, **318**, 426-430; (b) X. B. Yin and D. Y. Liu, *J. Chromatogr. A*, 2008, **1212**, 130-136.
15 S. Zhu, J. Zhang, S. Tang, C. Qiao, L. Wang, H. Wang, X. Liu, B. Li, Y. Li, W. Yu, X. Wang, H. Sun and B. Yang, *Adv. Funct. Mater*., 2012, **22**, 4732-4740.
16 (a) J. Zhou, Y. Yang and C. Y. Zhang, *Chem. Commun.*, 2013, **49**, 8605-8607; (b) Y. Xu, M. Wu, X. Z. Feng, X. B. Yin, X. W. He and Y. K. Zhang, *Chem-Eur. J.*, 2013, **19**, 6282-6288.
17 K. K. R. Datta, O. Kozak, V. Ranc, M. Havrdova, A. B. Bourlinos, K. Safarova, K. Hola, K. Tomankova, G. Zoppellaro, M. Otyepka and R. Zboril, *Chem. Commun*., 2014, **50**, 10782-10785.
18 B. Fahrenkrog and U. Aebi, *Nat. rev. mol. cell bio*., 2003, **4**, 757-766.
19 Y. Y. Zhang, M. Wu, Y. Q. Wang, X. W. He, W. Y. Li and X. Z. Feng, *Talanta*, 2013, **117**, 196-202.